

# Simulating the extent of the moderating influence of green space on urban climates

Meiring Beyers, Michael Roth  
*Klimaat Consulting & Innovation Inc., Guelph, Canada*  
*meiring.beyers@klimaat.ca, michael.roth@klimaat.ca*

15 June 2015

## Abstract

An understanding of the role of open space and vegetation to mitigate heat-related health risks is invaluable to urban designers and policy makers. However, these professionals may be prevented from introducing extensive urban green space in urban (re)design projects as it competes against conventional and tangible urban real estate development benefits. Therefore quantifying how specific green space layout and distribution characteristics may positively influence local and city wide climate is helpful to show benefits that are just as tangible. In this work, an urban climate simulation process and its results are described and illustrated by means of a case study in China that identifies the spatial influence of different green space scenarios. The simulation process described herein allows multiple city and green space forms to be evaluated for different climate zones to develop climate responsive design rules for green space area ratios, distribution and layout. In particular, the process allows the scoring of green space integration in city design by evaluating the relative temperature modification or offset provided by its introduction.

An urban climate simulation process is first described. The simulation process uses Open Source Computational Fluid Dynamic (CFD) tools to simulate city wide wind exposure for a proposed large scale city (re)development. These wind simulation datasets are coupled with typical annual hourly meteorology (TMY) data and a separate detailed solar exposure model and surface energy balance solver to predict the hourly climatic response for a given weather period. The computational solver and surface energy balance model also includes vegetation as porous moisture sources, so that the appropriate latent heat sink due to evapotranspiration and solar shading effects can be modelled. Ultimately, the process takes city geometry, vegetation plans and hourly meteorology data as input and delivers hourly surface and near-surface temperature maps. Using the simulation process, a city redevelopment case study is evaluated under varying green space distributions. Correlations between green space mitigation scenarios and the urban thermal response are presented and summarized in the findings.

## 1. Introduction

Urban form and layout, and in particular open space natural vegetation, can have a significant influence on the thermal characteristics of an urban neighbourhood. Urban planners and architects that aim to create more climate responsive or healthier city outdoor spaces, often require insight into the relative impact that different design interventions may have on local and city wide temperatures, thermal comfort and wind ventilation. Few tools exist that can provide a relative measure of such impacts at large enough scale to assess city scale

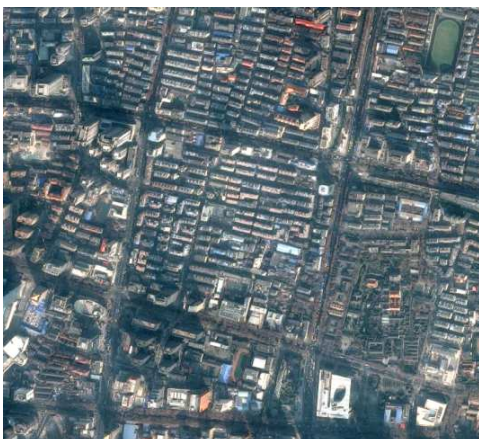


*Figure 1: A typical Chinese urban neighbourhood used in the modelling.*

design, with suitably high resolution to capture building and landscaping elements, but computationally fast enough to match the fast iterative design schedule of typical large scale city design projects. Here such a process is presented and applied to a generic case study in Nanjing, China.

Nanjing is located along the Yangtze River approximately 300 km from Shanghai. Nanjing is one of the three “Furnace Cities” in China along with Chongqing and Wuhan. The summer average temperature is 28°C with peak temperatures of 40°C. In summer, the combination of exposure to high solar radiation, high ambient temperatures, low wind speeds, and high humidity creates thermal conditions frequently perceived as uncomfortable to severely stressful. Maintaining the limited wind ventilation, providing solar shading, and encouraging vegetation evapotranspiration will therefore be important to improve the perceived thermal climate in the urban outdoor spaces. A typical urban form for China, the focus of the modeling below, is shown in Figure 1.

## 2. Methodology

The urban climate simulation process under development and applied here involves and combines a sequence of simulation steps to process, solve, and analyze the local microclimate for a three-dimensional urban geometry.

These steps include:

- Resolving the mean wind flow through an urban geometry using CFD;
- Simulating the hourly solar shading of the urban outdoor space;
- Calculating the urban ground thermal response as a function of the simulated wind and solar data fields, typical hourly meteorology data and land surface characteristics; and,
- Mapping seasonal climate statistics for thermal comfort, wind ventilation, and other metrics.

## 2.1 CFD wind simulations

For a three-dimensional urban geometry, 16 wind direction CFD simulations are performed to provide a mean wind data field to be used in the subsequent urban climate mapping. The Open Source CFD toolset OpenFOAM (Weller, et al. 1998) is used to pre-process the urban geometry and solve the 16 compass directions wind flows through the city. For a typical urban master plan climate analysis, the urban form is separated into site buildings, its surrounding buildings or terrain context, and various land surface classifications such as urban parks, roads, plazas, water bodies, or forests that may each have different material and thermal characteristics that influence ground temperature and associated perceived thermal comfort. For the current case study the modelled geometry and land surfaces used are shown in Figure 2. Figure 3 shows a typical computational grid with refinement of the urban core plan being evaluated.

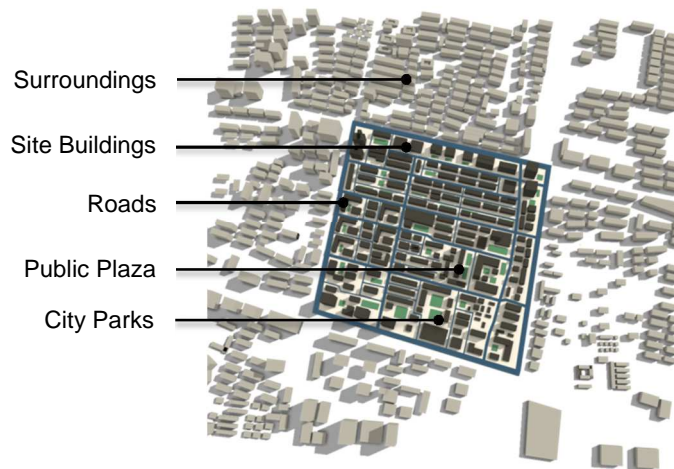


Figure 2: Modelled geometry and land use classifications.

For the CFD wind simulations, a steady state Reynold Average Navier-Stokes solver is used with the standard  $k - \epsilon$  turbulence model. The multiple wind direction CFD simulations are solved for a generic 10m wind speed (10m/s) to create a local velocity ratio data field that is coupled with the hourly meteorology data to estimate *in situ* hourly winds speeds. Figure 3 shows a typical pedestrian level wind speed distribution.

During the simulation a massless scalar species transport is solved to simulate the distribution of a water vapour source originating at each evaporating surface such as trees or grass surfaces. This tracer is subsequently used to identify the presence of an evaporative heat flux that influences the ground surface energy balance calculation.

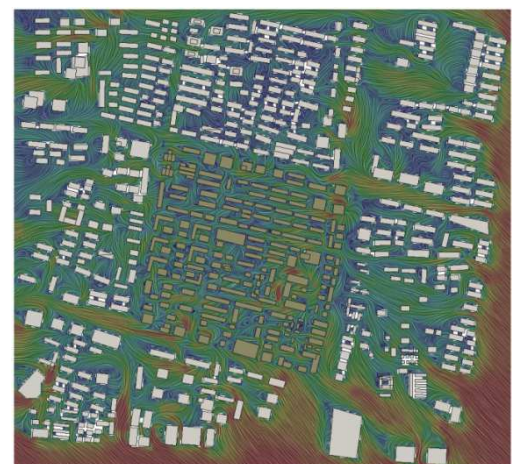
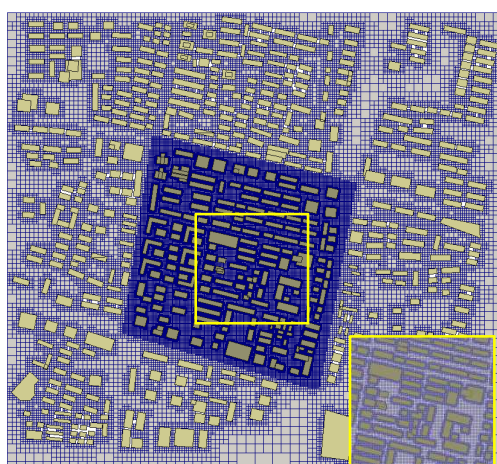


Figure 3: Computational mesh (left) and simulated pedestrian-level streamlines for a southeast wind (right).

## 2.2 Solar shading

A Python script solves the local hourly solar shading and sky view factor on a pedestrian level surface mesh, i.e. the analysis surface where the urban climate statistics will be mapped. The sky view factor and hourly shade map is used in the subsequent climate analysis to calculate the diffuse and direct solar radiation contributions received on the ground and at the pedestrian level analysis mesh where it influences the surface energy balance, the mean radiant temperature, and, ultimately, the local perceived temperature.

### 2.3 Surface energy balance, ground surface temperature, mean radiant temperature and perceived thermal climate

*Surface energy balance and ground surface temperature.* The hourly ground temperature is calculated on the surface mesh based on the TMY data input, the corresponding simulated wind velocity data field, the solar shading, and the sky view factor. To be able to perform a ground temperature calculation for a full annual hourly meteorology dataset (8760 hours), the force-restore method (Deardorff 1978) is applied. Surface material mass and thermal characteristics and leaf area index, where applicable, are stored on the analysis surface mesh based on the pre-processed geometry and land classifications. The ground temperature  $T_g$  is calculated according to

$$\frac{\partial T_g}{\partial t} = -\frac{c_1 H}{(\rho_s c_s d)} - \frac{c_2 (T_g - T_2)}{\tau_1} \quad (1)$$

where  $c_1 = 2\pi^{0.5}$  and  $c_2 = 2\pi$ .  $T_2$  is a restorative deep soil temperature approximated by the 24h average ambient temperature,  $\tau_1$  is a period of one day,  $c_s$  is the soil specific heat,  $d = (\kappa\tau_1)^{0.5}$  is the depth of the a diurnal temperature wave, and  $\kappa$  is the soil thermal diffusivity. The required ground surface energy balance is given by

$$H = \epsilon_g \sigma T_g^4 + H_s + LE_g - (1 - \alpha_g) S^\downarrow - \epsilon_g R^\downarrow \quad (2)$$

where  $\epsilon_g$  is the ground surface emissivity,  $\sigma$  is the Stefan-Boltzman constant,  $H_s$  is the sensible convective heat flux of the ground to atmosphere,  $L$  is the latent heat of evaporation,  $E_g$  is the local evaporation rate,  $\alpha_g$  is the ground albedo,  $S^\downarrow$  is incoming shortwave radiative flux,  $R^\downarrow$  is the downwelling longwave radiative flux. The nonlinear longwave radiation flux terms are linearized and the ground temperature equation discretized and numerically solved for 100s time intervals using the Crank-Nicholson method. The sensible convective heat flux is approximated by

$$H_s = \rho_a c_p C_H u_a (T_g - T_a) \quad (3)$$

where  $c_p$  is the air specific heat,  $C_H = 0.0025$  is the approximated surface heat transfer coefficient and  $u_a$  the local wind speed at pedestrian level. The surface energy balance applied in the force restore method includes the calculation of the latent heat sink due to evapotranspiration at relevant surfaces such as grass, forest and water bodies. The evapotranspiration heat flux at the ground surface is calculated according to the FAO Penman-Monteith method to estimate the reference crop evaporation (Allen, et al. 1998)

$$LE_g = \frac{\Delta(R - G) + K\rho_a c_p (e_s - e_a)/r_a}{\Delta + \gamma(1 + r_s/r_a)} \quad (4)$$

where  $R$  is the net incoming surface radiation,  $G$  is the soil heat flux,  $K$  is a unit time conversion factor,  $(e_s - e_a)$  represents the vapour pressure deficit of the air,  $\Delta$  represents the slope of the saturation vapour pressure temperature relationship, is the  $\gamma$  psychrometric constant and  $r_s$  and  $r_a$  are the bulk surface and aerodynamic resistances. To account for differences in plant canopy cover, the evapotranspiration heat flux is normalized with the reference grass leaf area index (2.88 m<sup>2</sup>/m<sup>2</sup>) and scaled to the relevant leaf area index (Pereira, S and Nova 2006) stored in the analysis surface mesh. The latent heat sink due to evapotranspiration (or water surface evaporation) is combined with shortwave and longwave solar radiation contributions and the convective (wind) heat flux to determine the ground surface temperature. A ground surface temperature field is generated on the analysis surface mesh for every hour of the typical meteorology year data. Hourly ground temperature data is then averaged and mapped for seasonal and daytime periods.

*Mean radiant temperature at pedestrian level:* The mean radiant temperature is subsequently calculated at every analysis surface mesh point based on the hourly short and long wave radiation data, the sky view factor and the solar shading factor computed in the solar shading solver, and the calculated ground temperature.

*Outdoor space perceived thermal climate:* The simulated hourly ground, mean radiant and ambient air temperature is subsequently used to calculate an equivalent or perceived temperature for the analysis mesh. The perceived temperature or thermal comfort index is calculated according to the Universal Thermal Climate Index (UTCI) methodology (Jendritzky, de Dear and Havenith 2012). The UTCI is an equivalent ambient temperature based on the physiological response of a reference person to the local environmental condition. The perceived temperature maps are generated for the site to identify how buildings, land surface, neighbourhood wind corridors, and green space may influence the local and site wide temperature distribution. Many different climate indicators, such as seasonal solar shading, wind ventilation metrics, etc. are created and mapped for different hourly and seasonal intervals. However, in this work the emphasis is on evaluating the summer averaged daily, afternoon, evening and night time perceived temperature distribution.

### 3. Nanjing master plan urban climate

#### 3.1 Case Study: Simulated urban climate for an urban neighbourhood in Nanjing, China

The methodology described above is applied to a case study for Nanjing. A number of different land surface treatments are tested here to evaluate the influence green space distribution may have on the local and neighborhood perceived climate. The tests included different road surface treatments (asphalt or concrete roads), different green space treatment at plazas between buildings (100% concrete to 40% vegetated open space) and different open park treatment (concrete to grass covered to tree-covered open parks). It is worth noting that the urban design code for Nanjing requires a minimum green space ratio of 35%. Table 1 summarises the different test cases evaluated for the master plan.

Table 1: Urban climate simulation test cases

Test	Road	Plaza	Parks	Other
0	Asphalt	100% concrete	100% concrete	No wind
1	Asphalt	100% concrete	100% concrete	
2	Asphalt	90% concrete, 10% grass	90% concrete, 10% grass	
3	Asphalt	80% concrete, 20% grass	80% concrete, 20% grass	
4	Asphalt	70% concrete, 30% grass	70% concrete, 30% grass	
5	Asphalt	60% concrete, 40% grass	60% concrete, 40% grass	
6	Asphalt	65% concrete, 35% grass	100% grass	
7	Asphalt	65% concrete, 35% grass	50% grass, 50% trees	
8	Concrete	65% concrete, 35% grass	50% grass, 50% trees	

Test 0 is a baseline worst case scenario where all urban terrain is concrete and roads are asphalt with no vegetation and no ventilating influence from the simulated wind field. Test 1 through 6 tests the influence of different public plaza treatments ranging from 100% concrete to 60% concrete and 40% vegetation (grass). Test 7 and 8 includes trees in place of grass for the vegetation within the city parks. Finally, Test 8 modifies Test 7 to include light-coloured concrete roads instead of asphalt. The material and thermal specifications used for different land surfaces and their combinations are shown in Table 2.

Table 2: Land surface material specifications

Bulk Surface	Albedo	Emissivity	Specific Heat	Thermal Conductivity	Density	Leaf Area Index	Solar Filter Ground	Solar Filter Human
Grass	0.25	0.95	1200	1.5	1200	2.88	0.7	0
Trees	0.25	0.95	1200	1.5	1200	5.0	0.7	0.7
Concrete	0.35	0.85	880	0.5	2200	0	0	0
Road	0.05	0.95	920	0.75	2200	0	0	0

For the ground surface calculation, bulk material and thermal properties are determined based on the combination of different ratios of hardscape or vegetation, where relevant. For vegetated surfaces, the ground properties for the temperature calculation are assumed to be medium-dry soil. For low-level vegetation types such as grass, a solar radiation filter is only applied to the ground temperature calculation and not to the mean radiant temperature experienced by people as low-level vegetation does not have a human shading benefit. For areas with trees, the solar shading filter is applied to both to the ground temperature and mean radiant temperature calculation to accommodate its solar shading effect on the ground and on people.

#### 3.2 Results and discussion

Given the very hot and humid climate conditions of Nanjing, the present discussion focus primarily on the summer averaged perceived climate. Figure 4 shows a typical set of perceived average thermal climate maps for the entire summer period for each of the different simulation tests. It is clear how the average local perceived temperatures are reduced as the green space ratio is increased. As per Figure 4, the local temperature change (reduction) between Test 1 and Test 8 ranges between 1°C (for road areas changed from asphalt to concrete) and 7°C (for city park areas changed from concrete to trees and grass). The influence and importance of resolving the simulated wind field to reduce the ground temperature and perceived temperature can also be seen in the difference between the temperature maps for Test 0 and 1. Also, outdoor spaces shaded by buildings is also approximately 2°C cooler compared to sun exposed areas such as the near east-west aligned streets that receive prolonged periods of direct solar radiation during summer days.

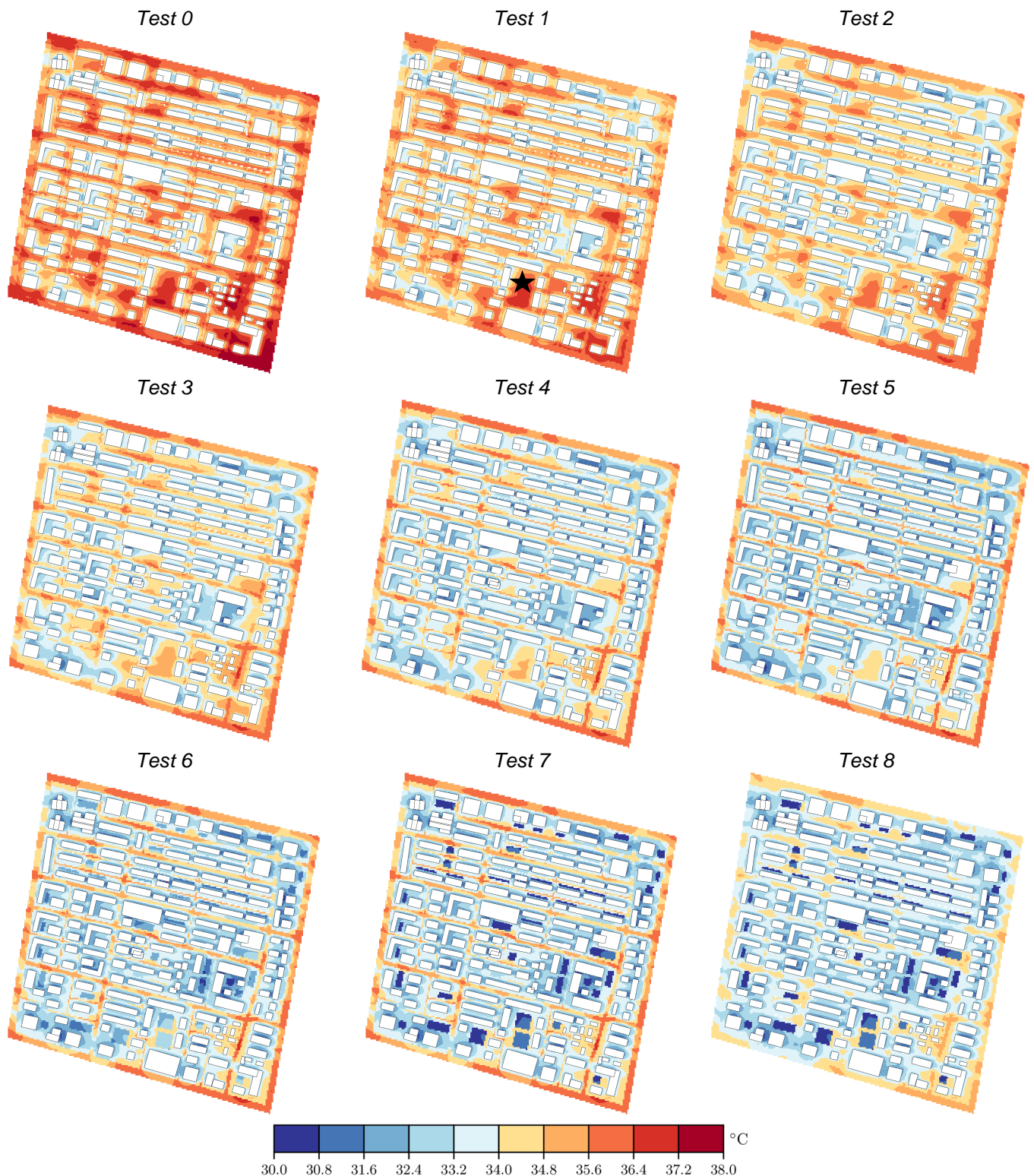


Figure 4: Simulated summer average perceived temperature (UTCI) map for the Nanjing urban plan. Site wide average temperatures are shown below in Figure 5. The black star on Test 1 indicates the plaza/green space area where the local average temperature is also compared in Figure 5.

Figure 5 shows the site wide weighted average of the mean perceived temperature for each of the tests performed. The site without any vegetation in parks and plazas and with asphalt roads has a mean summer perceived temperature of 35.2°C. Compared to that, the increased vegetation of the plaza open space changes the site average temperature to 34.7°C (Test 2) to 33.5°C (Test 5), for 10% to 40% vegetation, respectively. Further reducing grass cover and increasing the tree cover of the open space parks from 10% grass to 50% grass and 50% tree cover reduced the average site wide perceived temperature to 33.2°C. As shown in Figure 5, these reductions are similar but more pronounced for summer afternoon averaging periods when ground surface temperatures are highest. At night, the reduction is more limited due to the absence of solar radiation, with the benefits mainly due to the reduced thermal heat stored in the ground for the improved albedo and increased

vegetation of Test 8. Local temperature changes are more pronounced than what the site wide average temperatures may suggest. In Figure 8 the change in local daily average temperature at one plaza/city park where surfaces were changed from concrete to vegetated parks is shown in the dashed line. For pure concrete hardscape, the local temperature was 38°C. With increased vegetation (40% grass), the temperature was reduced to 34°C, close to the site wide average. A further increase in tree cover reduced the local temperature to 31°C. The range of perceived temperature differences modelled here for various urban land surfaces are similar to that measured and reported by Huang et al (2007), for Nanjing.

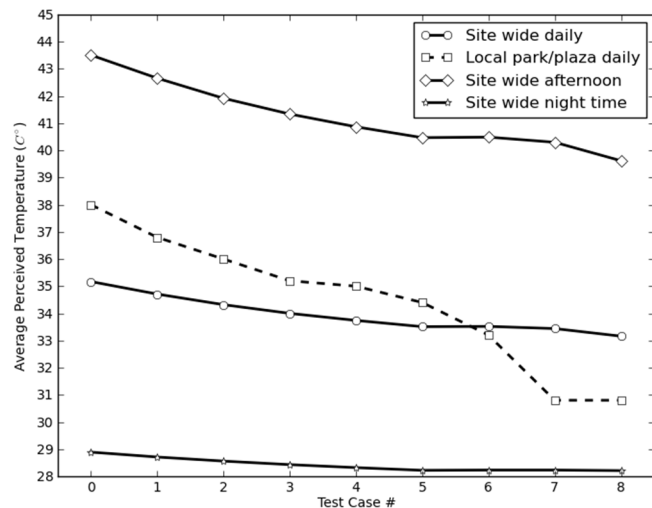


Figure 5: Mean daily, afternoon and night time perceived temperatures for the Nanjing urban plan.

#### 4. Conclusion

The work described here presented a city scale urban climate simulation process to test how city form, layout and land surface may influence local and site wide perceived temperatures. The work focused on a case study for Nanjing, China, given its hot summer climate and often dense urban neighbourhoods. The simulation process was applied to test how increases in public space vegetation and road surface specification may influence local and site wide city temperatures for a small, generic urban plan. For this study, perceived site wide average summer temperature was reduced by 2°C while local perceived temperatures in parks with increased vegetation decreased by as much as 7°C. Such reductions in site wide and local temperature may have very tangible benefits for the use and comfort of outdoor spaces. However and perhaps more importantly, it may have dramatic benefits for human health. As climate change increase regional and urban temperatures, cities will require better climate-resilient design strategies to offer shelter, especially during prolonged periods of intense heat. Public space parks and green space, wind ventilation landscape corridors, and building and city form and layout all contribute to an improved outdoor space climate.

The current "alpha" simulation process is under continuous development. The following enhancements are currently being evaluated, planned, or implemented:

- Improving the radiation solver to allow exchange between surfaces and varying building surface materials;
- Incorporating seasonality, e.g. changes in leaf area index;
- Adding a bucket model for precipitation and soil moisture in the force restore method for ground temperatures;
- Comparing and/or training of ground surface temperatures against both satellite products and field measurements; and,
- Comparing reductions in perceived temperatures against expected increases due to climate change

#### Acknowledgment

The authors would like to thank Ellen Lou, Anne Chen, and Kenichiro Suzuki of the urban design group of Skidmore, Owings & Merrill for their assistance with the Nanjing urban design code interpretation and translation and their continued innovative collaboration.

#### References

- Allen, RG, LS Pereira, D Raes, and M Smith. 1998. "Crop evapotranspiration: guidelines for computing crop water requirements." *FAO, Rome* **300** (9): D05109.
- Deardorff, JW. 1978. "Efficient prediction of ground surface temperature and moisture with inclusion of a layer of vegetation." *Journal of Geophysical Research* **83** (4): 1889-1903.
- Huang, L, J Li, D Zhao, and J Zhu. 2007. "A fieldwork study on the diurnal changes of urban microclimate in four types of ground cover and urban heat island of Naging, China." *Building and Environment* **43** (1): 7-17.
- Jendritzky, G, R de Dear, and G Havenith. 2012. "UTCI - Why another thermal index?" *International Journal of Biometeorology* **56** (3): 421-428.
- Pereira, AR, Green S, and NAV Nova. 2006. "Penman-Monteith reference evapotranspiration adapted to estimate irrigated tree transpiration." *Agricultural Water Management* **83** (1): 153-161.
- Weller, HG., G Tabor, H Jasak, and C Fureby. 1998. "A tensorial approach to computational continuum mechanics using object-oriented techniques." *Computers in Physics* **12** (6): 620-631.